agronomy

MDPI

Article

Exogenous Melatonin Alleviates the Inhibitory Effect of $NaHCO_3$ on Tomato Growth by Regulating the Root pH Value and Promoting Plant Photosynthesis

Yuanling Yang [1,†], Sihui Guan [1,†], Xiyao Jiang [1], Ming Li [2], Shaowei Wei [3] and Ming Diao [1,*]

[1] Key Laboratory of Special Fruits and Vegetables Cultivation Physiology and Germplasm Resources Utilization of Xinjiang Production and Construction Corps, Department of Agricultural College of Shihezi University, Shihezi 832003, China; 20222012046@stu.shzu.edu.cn (Y.Y.); guansihui@163.com (S.G.)
[2] Research Center of Information Technology, Beijing Academy of Agriculture and Forestry Sciences/National Engineering Research Center for Information Technology in Agriculture, Meteorological Administration-Ministry of Agriculture and Rural Affairs, Beijing 100097, China; lim@nercita.org.cn
[3] National Water Saving Irrigation Engineering Technology Research Center, Xinjiang Tianye Co., Ltd., Shihezi 832000, China; wsw062623@163.com
* Correspondence: diaoming@shzu.edu.cn
† These authors contributed equally to this work.

Abstract: Soil salinity is a severe threat to agricultural production. Most saline soils turn alkaline, increasing the soil pH and, in turn, hampering the growth and development of crops. In this study, the effects of a foliar spray of melatonin (MT; 100 μmol·L^{-1}) on the pH of the root environment, growth of tomato seedlings, endogenous MT levels, rapid chlorophyll fluorescence induction kinetics, and key enzymes of the Calvin cycle under alkaline (60 mmol·L^{-1} $NaHCO_3$) stress were studied in Riegel 87-5 tomatoes. The results revealed that the growth and photosynthesis of tomato seedlings were inhibited by increased pH in the root environment under alkali stress; however, the application of exogenous MT reduced the pH of the root environment, alleviated the inhibition of growth of tomato seedlings under alkali stress, increased the content of photosynthetic pigments, alleviated the damage of the donor and acceptor sides of the photosynthetic electron transport chain, increased the activity and efficiency of photosynthetic electron transport, and optimized the share of the light energy allocated to PSII reaction centers. Increased expression levels of Calvin-cycle enzymes, including fructose-1,6-bisphosphate aldolase (*FBA*), fructose-1,6-bisphosphate esterase (*FBP*), and phosphoglycerate kinase (*PGK*), led to enhanced photosynthetic performance in tomato seedlings. Exogenous MT boosted endogenous MT levels and stimulated the production and secretion of organic acids in the root system. This regulation of organic acid content reduced the environmental pH in the inter-root zone, alleviating the damage caused by alkali stress. This study indicated that the exogenous administration of MT may mediate an increase in endogenous MT levels, regulate the efficiency of photosynthesis and root pH levels, and play a crucial role in mitigating injury caused by alkali stress in tomato seedlings.

Keywords: melatonin; alkali stress; tomato; photosynthesis; Calvin cycle

Citation: Yang, Y.; Guan, S.; Jiang, X.; Li, M.; Wei, S.; Diao, M. Exogenous Melatonin Alleviates the Inhibitory Effect of $NaHCO_3$ on Tomato Growth by Regulating the Root pH Value and Promoting Plant Photosynthesis. *Agronomy* **2023**, *13*, 2777. https://doi.org/10.3390/agronomy13112777

Academic Editor: Sara Di Lonardo

Received: 13 October 2023
Revised: 3 November 2023
Accepted: 6 November 2023
Published: 8 November 2023

1. Introduction

Soil salinity is a commonly occurring abiotic stress. It poses a serious threat to the sustainability of agriculture and ecological and food security [1], particularly in arid and semiarid areas, severely affecting crop growth and development and yield formation. By 2019, more than 23% of the world's arable land resources were already affected by salinization [2]. Two types of salinity stress are salt stress and alkali stress [3]. Salt stress causes leaching of intracellular solutes and the accumulation of ions, ultimately leading to metabolic disorders and nutrient imbalances [4]. Alkali stress affects plants to a greater extent than salt stress [5]. Alkali stress affects the entire growth process of plants. Studies

have confirmed that the root system of a plant is the first to be affected by alkali stress. Large amounts of $NaHCO_3$ and Na_2CO_3 are present in soil under alkali stress, which can change the extracellular pH and affect the intracellular pH. This can trigger ionic toxicity and high pH in the soil environment, which interfere with the pH stability of the plant cells and disrupt a series of processes such as cellular metabolism [6], in particular, reducing photosynthetic performance and, thus, inhibiting growth [3]. Photosynthesis is a key determinant of crop yield and is highly susceptible to abiotic stresses [7]. Alkali stress disrupts the chloroplast membranes and the structure and function of photosynthetic organs; moreover, it reduces the photochemical efficiency of photosystem II (PSII) and the expression of photosynthesis genes, which leads to decreased plant photosynthesis [8]. Therefore, the adverse effects of alkali stress on plant photosynthesis can be ameliorated if the alkali tolerance of plants is improved.

Melatonin (N-acetyl-5-methoxytryptamine; MT) is a growth-regulating agent and antioxidant ubiquitously found in higher plants [9]. In plants, MT is chemically similar to the growth hormone IAA, which is involved in plant life activities such as seed germination, root growth, and flowering [10]. In addition, MT has the function of maintaining chlorophyll activity in plants [11], thus preventing leaf senescence. Studies have reported that exogenously applied MT and endogenous MT synthesized by the plant itself act in the same way, and both increase the tolerance of plants to stress [12]. Numerous studies have demonstrated that endogenous MT, as well as the application of exogenous MT, regulates various physiological and metabolic processes in plants [13] and is involved in the response to adverse abiotic stresses [14,15]. In oat, MT upregulates antioxidant genes and improves the photosynthetic capacity under osmotic stress [16]. In rice, MT alleviates the damage to rice seeds due to drought stress by increasing antioxidant enzyme activities [17]. In barley, low-temperature stress leads to the accumulation of oxidizing substances such as hydrogen peroxide (H_2O_2) and superoxide dismutase (SOD). The application of exogenous MT can regulate the changes in physiological indicators under cold-stress conditions, thus maintaining redox homeostasis. Additionally, exogenous MT has a role in regulating the circadian rhythm system. Furthermore, several studies have reported that MT can enhance stress tolerance in plants. Under stress, the application of exogenous MT can protect the photosynthetic system through various mechanisms. They include the promotion of PSII repair and electron transfer to balance the photosynthetic electron distribution and the increase in enzyme activities in the AsA-GSH cycle to reduce the oxidative damage to the photosynthetic apparatus due to reactive oxygen species (ROS) [18]. Moreover, MT can protect the photosynthetic system by maintaining the K^+/Na^+ balance and reducing ion toxicity [19]. Under alkali stress, exogenous MT can increase the stomatal opening of plant leaves [20], increase chlorophyll content [21], and reduce the destruction of photosynthetic proteins by ROS, which can effectively improve the photochemical efficiency of PSII [22].

Tomato (*Solanum lycopersicum* L.) is an essential vegetable crop that is widely cultivated and consumed globally. It is a moderately salt-sensitive crop and is highly susceptible to saline and alkaline stresses, which can cause severe yield loss. It has been demonstrated that MT reduces the decrease in the plant photosynthetic rate and balances PSII donor-side, acceptor-side, and reaction-center electron transfer rates to alleviate the adverse effects of salt stress on tomato seedlings [23]. However, studies on the effects of MT on tomato seedlings under alkali stress are scarce. Our previous studies have reported that exogenous MT can effectively alleviate the inhibition of growth and photosynthesis in tomato seedlings caused by alkali stress (60 $mmol \cdot L^{-1}$ $NaHCO_3$) [24]. However, the regulatory effects of MT on the pH, function, and structure of photosynthetic organs and on the expression of key genes of the Calvin cycle in tomato roots under alkali stress still need to be further investigated.

In this study, we aimed to elucidate the physiological photosynthetic mechanism of exogenous MT to alleviate alkali stress in tomato by investigating the role of MT in regulating the pH of tomato roots and the function and structure of photosynthetic organs under alkali stress. The present study employed the rapid chlorophyll fluorescence-induced

dynamics (OJIP) technique and the JIP-test analysis technique to rapidly analyze the energy capture of the PSII reaction center, the damage of PSII donor and acceptor sides, and the changes in electron transfer under adversity stress. Therefore, this study provides valuable information on the structure and function of plant photosynthetic organs and the determination of organic acid synthesis and secretion in the root system. Moreover, this study provides a theoretical basis for the use of MT as a growth regulator to improve the alkali tolerance of tomato.

2. Materials and Methods

2.1. Growth Conditions and Treatments

The test material was tomato variety "Riegel 87-5" (Seeds of this variety were provided by Vegetable Research Institute, Shihezi City, Xinjiang, China). The seeds were sterilized with 0.3% NaClO for 10 min, rinsed three times in sterile double-distilled water, and soaked in sterile double-distilled water (55 °C) for 15 min followed by a further soaking in sterile double-distilled water at 28 °C for 6 h. Finally, the tomato seeds were placed in an incubator at 28 °C for germination [25]. Seeds with a just-exposed radicle were selected and sown in 72-hole float trays containing peat: vermiculite = 2:1 (v/v) substrate. When the seedlings had grown to 3 leaves and 1 heart, well-grown seedlings with basic uniformity were selected, washed, and transplanted into buckets containing 12 L of Hogland nutrient solution (50% concentration) for precultivation for 7 d. The day and night temperatures in the greenhouse were 25–30 °C/15–18 °C, and the day and night-time durations were 16–17 h/7–8 h (no artificial light was supplemented). The seedlings were divided into four groups with varying treatments as follows: (1) control (CK): foliar spray of distilled water; (2) melatonin (CK + MT): foliar spray of 100 μmol·L^{-1} MT; (3) alkali stress (N): $NaHCO_3$ stress treatment and foliar spray of distilled water; (4) application of MT under alkali stress (N + MT): $NaHCO_3$ stress treatment and foliar spray of 100 μmol·L^{-1} MT. $NaHCO_3$ was applied at a concentration of 60 mmol·L^{-1} and added directly to the nutrient solution. MT was applied as a foliar spray using a misting sprayer at 8:30 pm each day until water droplets fell from the leaves (approximately 5 mL per plant). The concentrations of $NaHCO_3$ and MT used in the experiment were determined based on the pretest screening. The seedlings in the four groups were supplied with oxygen using 24 h oxygen pumps during the whole period, and the nutrient solution was replaced every 3 days to ensure adequate nutrient supply for plant growth. The experiment was a one-way completely randomized block design, with 18 seedlings per treatment and 3 replicates. The indexes were measured after 9 days of treatment.

2.2. Assessment of Various Indexes

2.2.1. Measurement of Growth Indicators

Plant height was determined by measuring the distance from the root base 1 cm below the cotyledons to the growing point of the seedling using a tape (in cm). Fresh and dry weights of aboveground and belowground parts were determined as follows: The plant surface and roots were washed with deionized water and dried using a filter paper. The aboveground and belowground parts were quickly weighed (fresh weight) on a balance (Thermo Fisher, Waltham, MA, USA). Further, the aboveground and belowground parts were separately placed in paper bags and dried in an oven at 105 °C for 20 min, followed by drying at 75 °C until constant weight was obtained. The dry weight was measured on the balance, and the root-to-shoot ratio was calculated according to the following formula:

$$\text{Root-to-shoot ratio (R/S)} = \text{belowground dry weight/aboveground dry weight} \quad (1)$$

2.2.2. Endogenous MT Levels

To extract MT, 0.1 g of leaf sample was mixed with 1 mL of 80% methanol. The mixture was ground, incubated overnight to allow extraction, and centrifuged. The supernatant was filtered using a needle filter. Using this, the endogenous MT level was determined using

high-performance liquid chromatography (HPLC). The chromatographic instrument was a RIGOL L3000 high-performance liquid chromatograph with the Shimadzu fluorescence detector RF-20A; excitation wavelength 280 nm; emission wavelength 348 nm; chromatographic column: RIGOL C18 reversed-phase chromatographic column (250 mm × 4.6 mm, 5 μm); column temperature: 30 °C; flow rate: 0.8 mL·min^{-1}; and injection volume: 10 μL. For the mobile phase, solvent A was methanol and B was 0.1% formic acid solution. It was run according to the following gradient: 0–10 min, A: 10%; 10–30 min, A: 10–50%; 30–35 min, A: 50–10%; 35–45 min, A: 10%.

2.2.3. Determination of pH and Organic Acid Content in the Root Environment

By referring to the method by Gao et al. [26], the pH value was determined by taking the supernatant of the collected liquid after 8 h.

Total organic acid content was determined by referring to the method by Zhang et al. [27]. To 20 mL of the supernatant of the collection solution into a beaker, 2 drops of 1% phenolphthalein indicator were added, and titration was performed with 0.01 mol·L^{-1} NaOH until the point where the color just changes and does not fade within 15 s. The amount of NaOH required for this end point was recorded. The titration was repeated 3 times, and the average was calculated. The total organic acid content was calculated according to the following formula:

$$\text{Total organic acid (mg/g·FW}^{-1}) = V \times C \times (R/W) \times (B/A) \times 1000 \quad (2)$$

where A, B, C, V, and W indicate grams of sample (g), total volume of sample extract (mL), concentration of NaOH solution (mol·L^{-1}), volume of NaOH used (mL), and volume of filtrate taken during titration (mL), respectively. R was considered to be −0.045.

To determine the content of individual organic acids (oxalic acid, malic acid, citric acid, and succinic acid), first, 1 g of root sample was rapidly ground in liquid nitrogen. To this, 10 mL of sterile double-steaming water extract was added, filtered with 0.22 μm aqueous membrane 3 times, and stored at −40 °C. To prepare 1000 mg·L^{-1} stock solutions of each standard organic acid, ultrapure water was added to dissolve 10 mg of oxalic acid, malic acid, citric acid, and succinic acid (Sigma; purity > 99.5%), respectively, and the volume was made up to 10 mL. Concentration gradients of each acid were prepared using the standard stock solution, and the standard curve was plotted (see Table 1). To determine the content of each organic acid, reverse-phase high-performance liquid chromatography (RT-HPLC) was used. HPLC liquid-phase conditions were as follows: chromatographic column, Thermodyncronis C18 (4.6 mm × 250 mm, 5 μm); mobile phase, 0.1% methanol (chromatographic grade; Sinopharm Chemical Reagent Corporation, Jiangsu Province, China); flow rate, 1 mL·min^{-1}; column temperature, 40 °C; injection volume, 20 μL; and detection wavelength, 210 nm.

Table 1. Organic acid regression equations and correlation coefficients.

Organic Acid	Regression Equation	Correlation Coefficient
oxalic acid	Y = 57,711.33x + 91.14	R = 0.999
malic acid	Y = 613.1733x + 0.3166	R = 0.999
citric acid	Y = 654.123x − 1.71992	R = 0.999
succinic acid	Y = 386.08x + 3.0225	R = 0.999

2.2.4. Chlorophyll Content

The leaves were extracted with 95% ethanol for 48 h in dark. The absorbance (A) of the extracts was measured at 665, 649, and 470 nm. The contents of chlorophyll a, chlorophyll b, chlorophyll (a + b), and carotenoid were calculated by referring to the method by Yanlu and Xinsheng [28]:

$$\text{Chlorophyll a content (Chl a)} = 13.95A_{665} - 6.8A_{649} \quad (3)$$

$$\text{Chlorophyll b content (Chl b)} = 24.96A_{649} - 7.32A_{665} \quad (4)$$

$$\text{Chlorophyll a + b content (Chl a + b)} = 18.16A_{469} + 6.63A_{665} \quad (5)$$

$$\text{Carotenoid content} = (1000A470 - 2.05C_a - 114.8C_b)/248 \quad (6)$$

$$\text{Chloroplast pigment content} = (C \times V \times N)/W \quad (7)$$

where C is the pigment content ($mg \cdot L^{-1}$), V is the volume of extract (L), N is the dilution factor, and W is the fresh weight of the sample (g).

2.2.5. Photosynthetic Gas-Exchange Parameters

The 4th functional leaf (counted from the bottom to top) of the tomato seedlings was selected for the determination of photosynthetic gas-exchange parameters using a Li-6800 portable photosynthesizer (Li-COR, Lincoln, NE, USA) during 10:00–12:00 on the 9th day after treatment. The photosynthetic gas-exchange parameters measured were net photosynthetic rate (Pn), stomatal conductance (Gs), intercellular CO_2 concentration (Ci), and transpiration rate (Tr). Each treatment was repeated three times, and each replicate was measured five times. The measurement environment was as follows: temperature of 25 °C, light intensity of 1000 ± 10 $\mu mol \cdot m^{-2} \cdot s^{-1}$, and an atmospheric CO_2 concentration of 350 ± 5 $\mu mol \cdot mol^{-1}$.

2.2.6. Rapid Chlorophyll Fluorescence-Induced Kinetics (OJIP) Curve Measurement and JIP-Test Parameters

After 2 h of incubation in the dark, OJIP curves were assessed and plotted for the 4th functional leaf under saturated pulsed light (5000 $\mu mol \cdot m^{-2} \cdot s^{-1}$) using the M-PEA Multifunctional Plant Efficiency Analyzer (Hansatech, Birmingham, UK). Fluorescence signals were recorded until the end of 3 s, and the initial rate of recording was 1×10^5 data points per second. The JIP test was performed by referring to the method by Schansker [29]. The JIP-test parameters and formulae for their calculation are shown in Table 2.

Table 2. Parameters and formulae for their calculation used in the JIP-test analysis.

Parameters and Formulae	Definition
F_o	Minimal recorded fluorescence intensity
F_m	Maximal recorded fluorescence intensity
$F_v = F_m - F_o$	Variable fluorescence
PI_{total}	Performance index
RC	Reaction center
CS_m	Cross-section of the sample ($t = t_{fm}$)
ABS/RC	Absorption flux per RC
TR_o/RC	Trapped energy flux per RC
ET_o/RC	Electron-transport flux per RC
DI_o/RC	Dissipated energy flux per RC
TR_o/CS_o	Trapped energy flux per *CS* at $t = t_o$
ET_o/CS_o	Electron-transport flux per *CS* at $t = t_o$
DI_o/CS_o	Dissipated energy flux per *CS* at $t = t_o$
ABS/CS_o	Absorption flux per *CS* at $t = t_o$
RC/CS_O	Density of reaction centers per cross-section (at $t = t_o$)
S_m	The normalized area between the J–P phase and the line $F = F_m$
φP_o	Maximum photochemical efficiency of PSII (at t = 0)
φE_o	Quantum ratios of PSII electron transfer (at t = 0)
φR_o	Quantum efficiency of PSI receptor-side terminal electron-acceptor reduction
δR_o	Reflects the efficiency of individual electrons traveling from the electron-transport chain between PSI and PSII of the photosystem to the terminal electron acceptor on the receptor side of PSI
M_o	Maximum rate at which Q_A is reduced

2.2.7. Determination of the Expression of Key Genes of Photosynthetic Carbon Assimilative Enzymes

In total, 0.2 g of fresh tomato leaves was rapidly preserved in liquid nitrogen for *RNA* extraction and gene expression analysis. Total *RNA* was extracted using an *RNA* microextraction kit and purified using an *RNA* purification kit. The first strand of *cDNA* was synthesized using a reverse-transcription kit and used as a template for real-time quantitative PCR (RT-qPCR). RT-qPCR was performed in the iQ multicolor real-time quantitative PCR detection system. The 20 μL reaction system for reverse transcription contained the following: 2 μg total *RNA*, 2 μL 8 × g*DNA* remover, and 16 μL RNase-free ddH_2O. For RT-qPCR, the reaction mixture contained 1 μL of *cDNA*, 0.4 μL of each upstream and downstream primer, and 18.2 μL of the fluorescence quantification mix. The RT-qPCR reaction procedure was as follows: pre-denaturation at 95 °C for 3 min; denaturation at 95 °C for 30 s; and 40–45 cycles of denaturation at 95 °C for 3–10 s followed by annealing and extension at 60 °C for 10–30 s. Fluorescence data were collected at the end of the annealing step of each cycle. The actin gene of tomato was used as an internal reference gene. Relative gene expression levels were calculated as described previously [30].The experiment involved three replicates. The specific primer sequences used to amplify the genes are shown in Table 3.

Table 3. Genes and primers analyzed by real-time quantitative PCR.

Gene	Gene-ID	Sequence of Forward Primer	Sequence of Reverse Primer
RCA	LOC101250725	TTGGACGGATTCTACATCGC	CTCCCCAAACACCCAAAATAAG
PGK	LOC101253805	GAAGAGCGTTGGAGACCTTAG	AGTGTTTGATGGTAGGGATGG
GADPH	LOC100736499	ACTCTGGTATATGTGTTACTC	AGGGAAGCAAGATTACTAAA
SBP	LOC100316873	AGAAATACACCTTGAGATACACCG	TCAAGAATCCTAACGGTGCC
FBP	LOC101264273	AATTTCCATCTCTTCCCCACC	TCGGTTTCTTGATCTGTGCTG
FBA	LOC1181999	CTGTATGGACCGATGGACTTAC	AAGGTCTAAAGGGTAAGCTACATAAG

2.3. Data Analysis

Microsoft Office Excel 2010 (Microsoft Corporation, Washington, DC, USA) software was used for the data analysis. SPSS 19 (IBM Corporation, Chicago, IL, USA) and The R Programming Language (University of Auckland, New Zealand) software were used for data analysis and for plotting graphs. One-way analysis of variance (ANOVA) was used to test the mean value of each treatment using Duncan's multiple polarity method. The least-significant difference method (LSD) was used to analyze the significance of the differences between the different treatments ($p < 0.05$).

3. Results

3.1. Growth Traits, Biomass, and Endogenous MT Levels

Compared with CK, $NaHCO_3$ treatment (N) had a significant inhibitory effect on the growth of tomato seedlings, as evidenced by a smaller crown size (Figure 1A) and a significant reduction in the plant height, root–crown ratio, and dry and fresh weights of above-ground and below-ground parts, whereas foliar spraying of exogenous MT (N + MT) alleviated the inhibitory effect of $NaHCO_3$ stress on the growth of tomato seedlings (Figure 1C–H).

As can be seen from Figure 1B, the endogenous MT content following CK treatment was low at 87.24 $ng \cdot g^{-1}$, whereas $NaHCO_3$ stress resulted in increased endogenous MT content. In addition, the addition of exogenous MT induced an increase in endogenous MT levels under both $NaHCO_3$ stress and no-$NaHCO_3$ stress conditions, and the endogenous MT content was significantly higher in the CK + MT treatment than in the N + MT treatment.

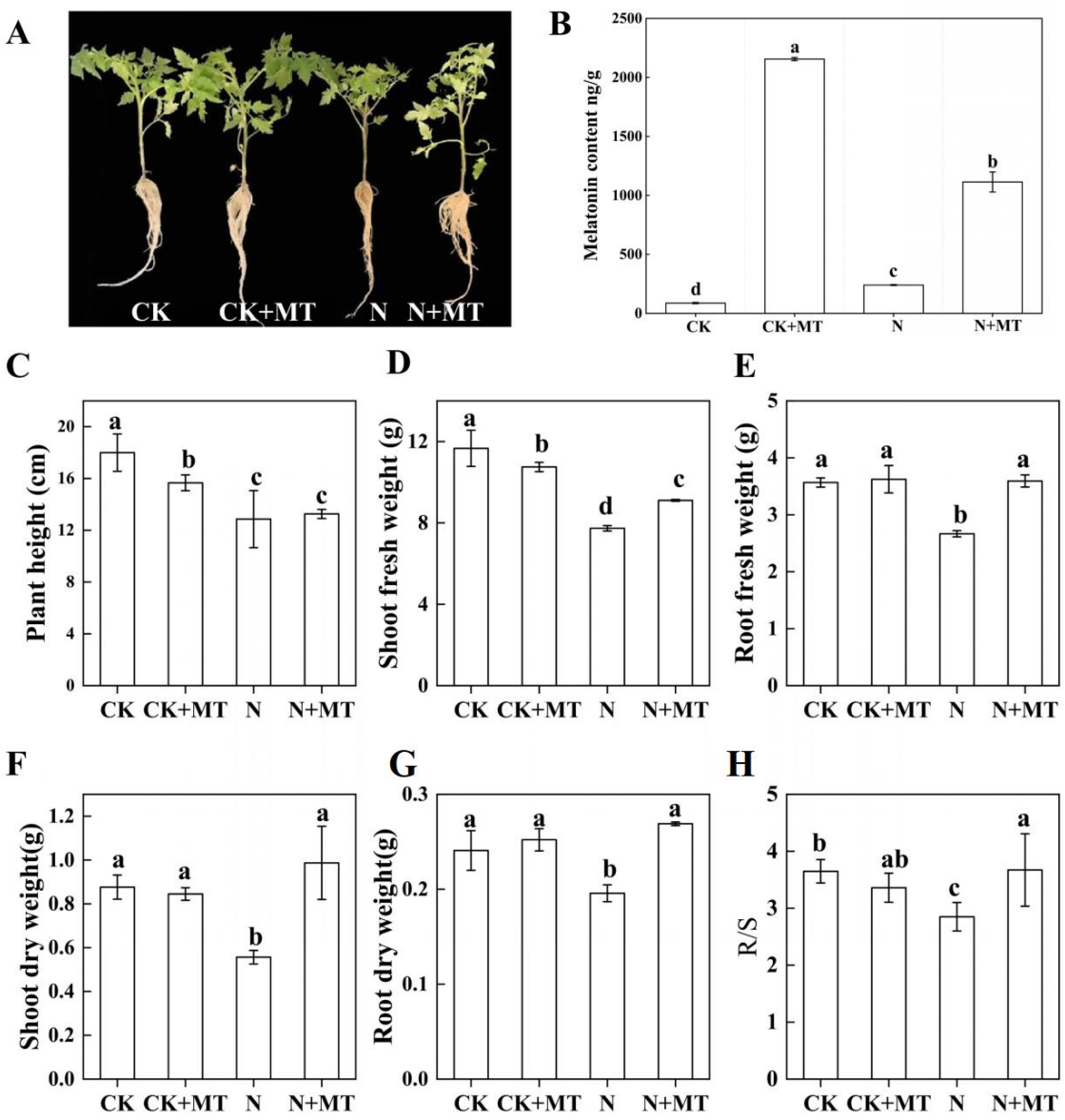

Figure 1. Effect of $NaHCO_3$ stress and exogenous MT treatment on the phenotypic traits and biomass of tomato seedlings. (**A**) The phenotypes of tomato seedlings under different treatments. (**B**) Content of endogenous MT in the leaves of tomato seedlings. (**C**) Plant height. (**D**) Fresh weight of aboveground parts. (**E**) Fresh weight of belowground parts. (**F**) Dry weight of aboveground parts. (**G**) Dry weight of belowground parts. (**H**) Root-to-shoot ratio. Each value represents the mean ± SE of three replicates. Different letters indicate significant differences between treatments ($p < 0.05$) in all figures.

3.2. pH of the Root Environment

Figure 2A shows the inter-root pH at 8 h of root secretion at d 9 under different treatments. As can be seen from Figure 2A, the N treatment significantly increased the inter-root pH to 8.57, whereas both CK and N + MT significantly reduced the inter-root pH to varying degrees compared with CK and N treatments, respectively. Thus, MT application reduced the inter-root pH under alkali stress to some extent.

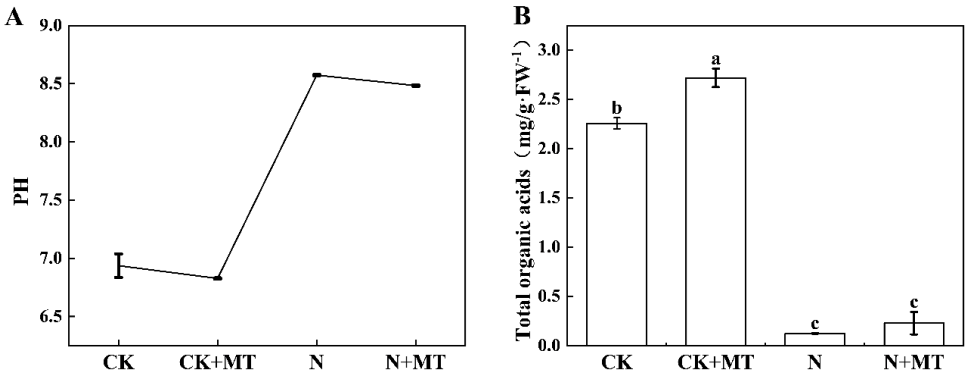

Figure 2. Changes in pH and organic acid contents in tomato roots under $NaHCO_3$ stress. Changes in (**A**) pH; and (**B**) total organic acids. Different lower−case letters indicate significant differences between treatments ($p < 0.05$).

Total organic acid contents were substantially reduced by 96% and 92% in N and N + MT compared with CK and CK + MT groups, respectively (Figure 2B). The organic acid content increased by 50% in the N + MT group compared with that in the N group. This indicated that MT reduced the root pH by increasing the secretion and synthesis of organic acids in the root system, thereby alleviating the effect of alkali stress in tomato.

Under unstressed conditions (CK and CK + MT treatments), the dominant organic acid was oxalic acid, followed by succinic acid. Therefore, oxalic acid was the main organic acid synthesized and secreted by the tomato root system. After N treatment, the oxalic acid content was significantly reduced by 67.32%, whereas that of succinic acid, citric acid, and malic acid significantly increased compared with CK. The increase in oxalic acid synthesis facilitated the secretion of oxalic acid, leading to its continuous accumulation in the culture broth. After N + MT treatment, the oxalic acid content was significantly increased by 136%, whereas that of malic and citric acid was reduced by 22.56% and 20.04%, respectively (Figure 3). Thus, the changes in organic acid synthesis and secretion in the presence of $NaHCO_3$ were attributed to both Na^+ and HCO_3^-.

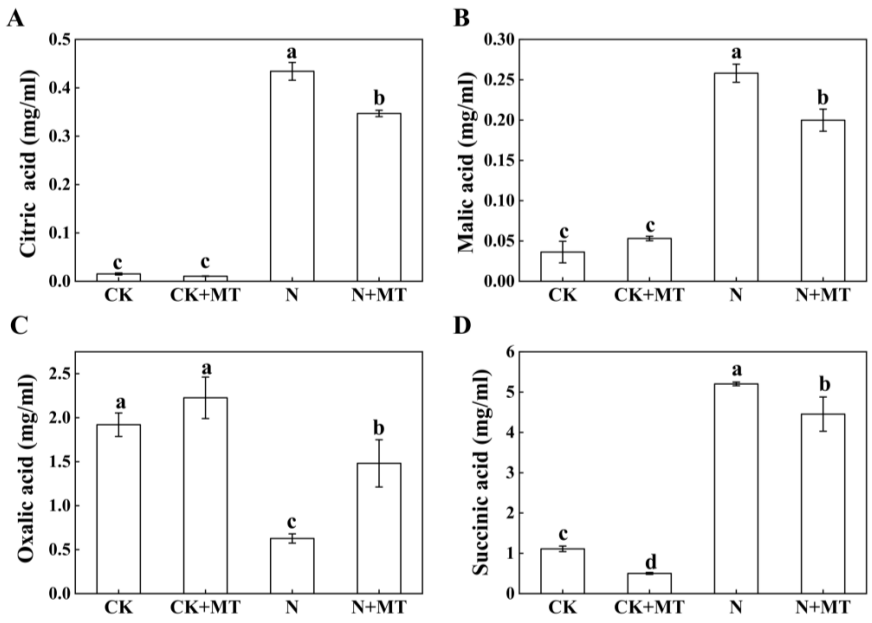

Figure 3. Organic acid content in the root system of tomato seedlings under $NaHCO_3$ stress conditions. The contents of (**A**) citric acid, (**B**) malic acid, (**C**) oxalic acid, and (**D**) succinic acid. Different lowercase letters indicate significant differences between treatments ($p < 0.05$).

3.3. Chlorophyll Content

Chl a, Chl b, total chlorophyll, and carotenoid contents were significantly increased by 20.45%, 17.76%, 19.70%, and 26.62%, respectively, in the CK + MT group compared with the CK group (Figure 4). They were reduced by 40.90%, 40.38%, 40.89%, and 19.74%, respectively, in the N group compared with the CK group. This indicated that $NaHCO_3$ stress resulted in a reduced content of photosynthetic pigments in the leaves of tomato seedlings. The N + MT treatment significantly increased the contents of Chl a, Chl b, carotenoids, and total chlorophyll by 28.44%, 25.90%, 21.69%, and 27.73%, respectively, compared with the N treatment. This indicated that MT application maintained high photosynthetic pigment content under alkali stress.

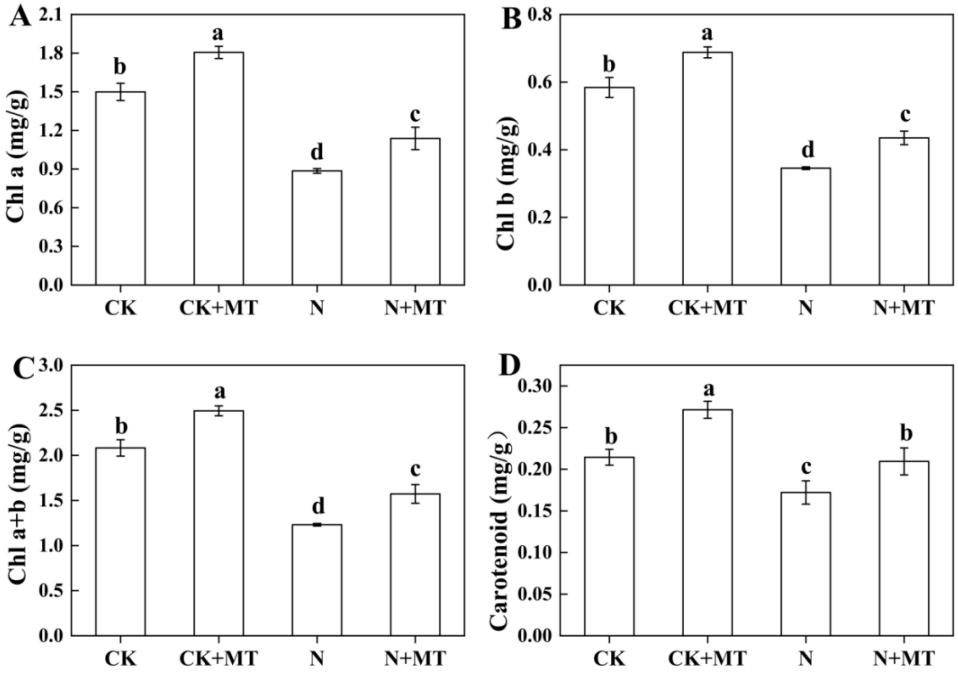

Figure 4. Effect of $NaHCO_3$ stress and exogenous MT treatment on (**A**) Chl a(Chlorophyll a content), (**B**) Chl b(Chlorophyll b content), (**C**) Chl a + b(Chlorophyll a + b content), and (**D**) carotenoid content in the leaves of tomato seedlings.

3.4. Photosynthetic Gas-Exchange Parameters

In the N group, photosynthesis in the leaves of tomato seedlings was decreased, as reflected by the significant decrease in Pn, Gs, Ci, and Tr by 54.65%, 47.88%, 106%, and 63.23%, respectively, compared with the CK group. Compared with the N treatment, the N + MT treatment alleviated the effects of alkali stress on the above parameters to varying degrees; Pn, Gs, Ci, and Tr were significantly increased by 50.55%, 57.49%, 33.14%, and 93.4%, respectively (Figure 5). This indicated that MT application could alleviate the unfavorable effects of $NaHCO_3$ stress on the photosynthesis in the leaves of tomato seedlings.

3.5. OJIP Curves

Figure 6A shows the OJIP curves between the O-phase (F_o) and the P-phase (F_o) under various treatments. Compared with the CK treatment, the amplitude of I–P of the OJIP curves under the CK + MT treatment gradually increased, particularly at the highest amplitude of the CK + MT treatment. Under the N treatment, the O phase was increased; the P phase was decreased; the amplitude of I–P was decreased, and the OJIP curves were distorted and became flat. Compared with the N treatment, the N + MT treatment increased the amplitudes of the P phase, I–P, and O–P.

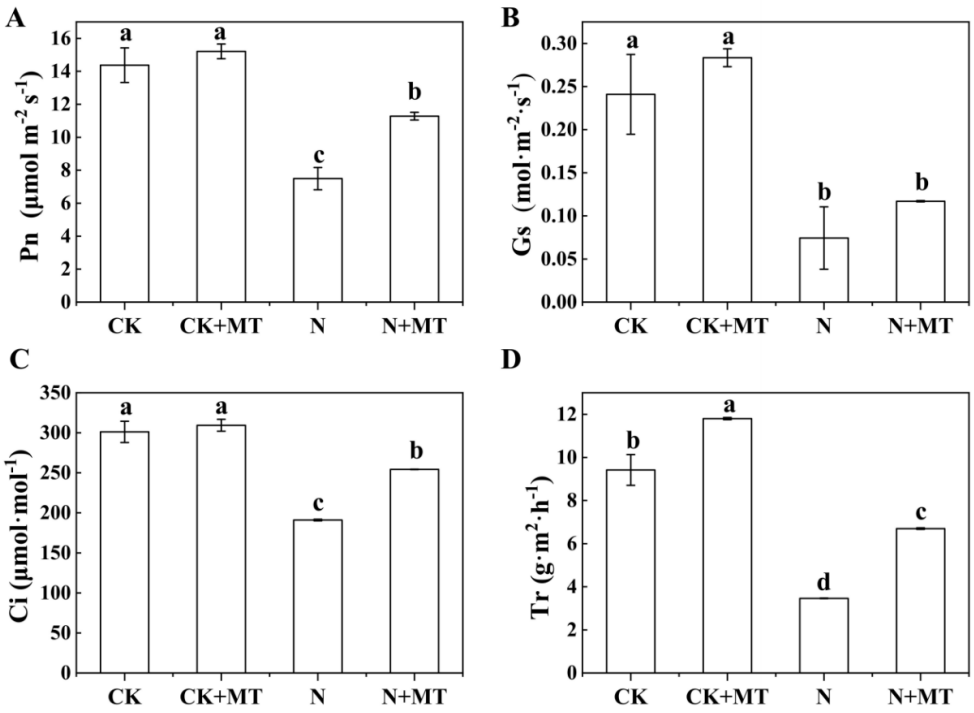

Figure 5. Effect of $NaHCO_3$ stress and exogenous MT treatment on the photosynthetic gas−exchange parameters in the leaves of tomato seedlings. (**A**) Photosynthetic rate (Pn). (**B**) Stomatal conductance (Gs). (**C**) Intercellular carbon dioxide concentration (Ci). (**D**) Transpiration rate (Tr).

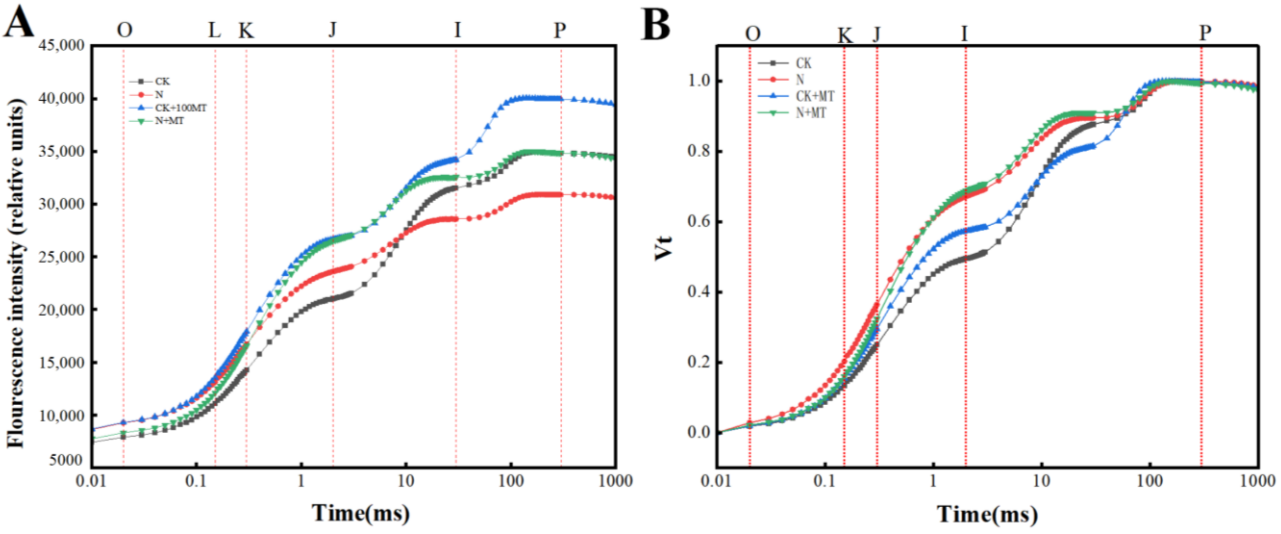

Figure 6. Effect of exogenous MT application on fast-fluorescence kinetic curves of tomato seedlings under $NaHCO_3$ stress. (**A**) OJIP curve. (**B**) Vt curve. In (**A**,**B**), O: fluorescence at t = 20 μs; K: fluorescence at t = 300 μs; J: fluorescence at t = 2 ms; I: fluorescence at t = 30 ms; P: fluorescence at t ≈ 300 ms.

The effects of exogenous MT application on the O–J, J–I, and I–P phase processes in the OJIP curves of the leaves under various treatments were further analyzed, and the sites of action of the PSII electron-transport chain were identified. The values of the chlorophyll transient fluorescence intensity under various treatments were double-normalized and displayed as the relative variable fluorescence [V_t, $V_t = (F_t - F_o)/(F_m - F_o)$] at any moment (where F_t is the fluorescence value at any moment) (Figure 6B). In the CK + MT group, the V_t increased between the K–J phases compared with the CK group. Vt between K–J and J–I was increased under the N treatment, indicating that the oxygen-excreting complex (OEC)

was damaged. The difference in the K–J phase was not significant in the N + MT treatment compared with that for the N treatment.

3.6. JIP-Test Parameters

The specific-activity parameter of PSII reflects the magnitude of activity of photosynthetic organ structures and compares the state superiority of photosynthetic structures under different treatments by the quantum efficiency of the active-unit reaction center (RC) and the unit light-exposed area (CS). ABS/RC, TR_o/RC, DI_o/RC, RE_o/RC, and PI_{total} were increased by 14.65%, 24.74%, 12.22%, 74.31%, and 52.83%, respectively, and the energy transferred (ET_o/RC) was decreased by 13.80% in the CK + MT treatment compared with the CK treatment (Figure 7A). Under the N treatment, ABS/CS_o, TR_o/CS_o, ET_o/CS_o, RE_o/CS_o, PI_{total}, and S_m values were decreased, with S_m decreasing by 33.86%. ABS/CS_o, TR_o/CS_o, M_o, and S_m values were increased to varying degrees under the N + MT treatment compared with the N treatment.

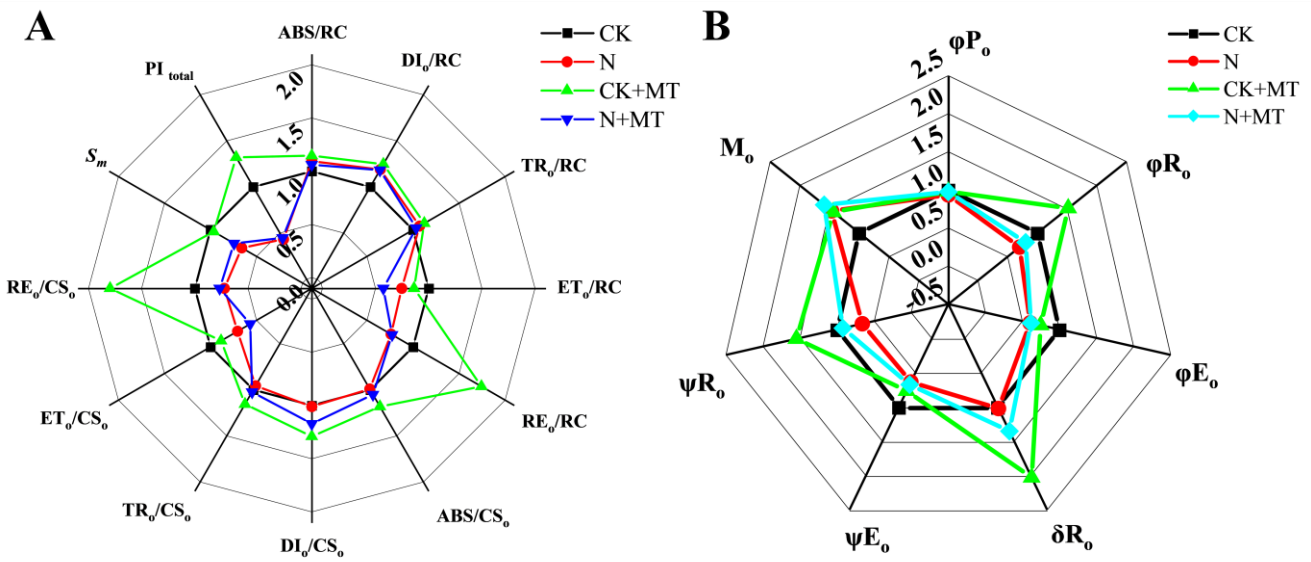

Figure 7. (**A**,**B**) are both PSII specific activity parameters.

When t = 0, ψE_o reflects the efficiency with which a single exciton captured by the active reaction center drives the transfer of electrons other than Q_A. That is, ψR_o is the efficiency of a single exciton captured by an active reaction center to drive a single electron from Q_A^- through the electron-transport chain to the terminal electron acceptor on the PSI-receptor side. The CK + MT treatment significantly increased the ψR_o and M_o values compared with the CK treatment, with ψR_o increasing by 41.13% (Figure 7B). However, the values of φR_o, φE_o, ψE_o, and ψR_o were decreased under the N treatment by 33.90%, 36.63%, 29.71%, and 33.90%, respectively. The values of M_o and δR_o were significantly increased, with Mo increasing by 46.4%. The values of φR_o, ψE_o, φE_o, and ψR_o were significantly increased by 43.01%, 6.4%, 6.4%, and 39.54%, respectively, but the M_o value decreased by 8.6% under the N + MT treatment compared with the N treatment.

3.7. Expression of Key Genes for Photosynthetic Carbon Assimilation Enzymes

Figure 8 shows the relative transcript levels of six genes encoding key enzymes for carbon assimilation. As can be seen from Figure 8, the relative transcript expression levels of four genes, *FBA*, *PGK*, *RCA* and *SBP*, were increased under CK + MT treatment compared with CK treatment, by 121.88%, 123.81%, 63.89% and 67.88%, respectively; the $NaHCO_3$ treatment downregulated the relative expression levels of the *FBA* and *GADPH* genes but increased the relative transcript expression levels of the rest of the genes coding for the relative transcript expression levels of key carbon assimilation enzyme genes. Compared

with the N treatment, the N + MT treatment increased the expression levels of the *FBA*, *FBP*, and *PGK* genes by 46.61%, 6.85%, and 146.22%, respectively.

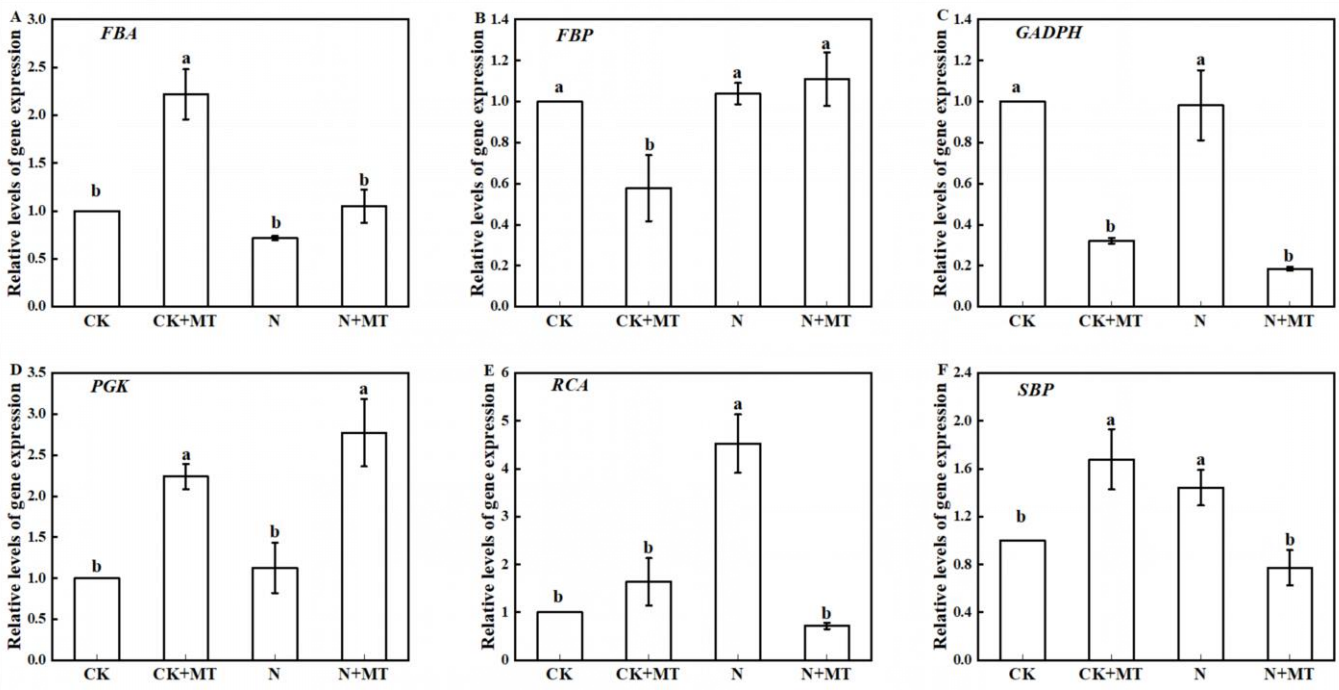

Figure 8. Changes in the expression of transcript levels of six genes affected by MT in the leaves of alkali-stressed tomato seedlings. (**A**) *FBA* (fructose-1,6-bisphosphate aldolase gene; (**B**) *FBP* (fructose-1,6-bisphosphate esterase gene; (**C**) *GAPDH* (3-phosphoglyceraldehyde dehydrogenase gene; (**D**) *PGK* (Phosphoglycerate kinase gene; (**E**) *RCA* (Rubisco activase gene); and (**F**) *SBP* (sedoheptulose-1,7-bisphosphate esterase gene transcripts were quantified by quantitative PCR and measured relative to actin transcripts.

4. Discussion

In recent years, MT has been widely recognized for its ability to improve resistance to abiotic stresses in plants. For example, in drought stress, exogenous MT application can alleviate drought stress by reducing the ROS content, thereby increasing fruit yield [31]. In the context of heavy-metal stress, MT treatment increases the synthesis of secondary metabolites, thereby alleviating nickel-induced growth inhibition [32]. Furthermore, MT can alleviate the effects of salt stress by enhancing the AsA-GSH cycle to increase stomatal conductance, thus modulating the expression of salt-tolerance-related gene [33]. MT and hydrogen sulfide have been reported to synergistically regulate salt-stress tolerance [34]. In this study, we analyzed the effect of MT on the pH of the root environment under $NaHCO_3$ stress and the mechanisms of regulation of the structure and performance of the photosynthetic apparatus in tomato seedlings.

4.1. Effect of Exogenous MT on Growth and Endogenous MT Levels in Tomato Seedlings under $NaHCO_3$ Stress

Salt and alkali stresses change the morphological structure and physiological and biochemical functions of plants, thus hindering the normal growth and development of plants and even causing death in severe cases. Increases and decreases in biomass are important indexes for evaluating the response of plants to saline and alkali stresses. Our results indicated that exogenous MT application could promote the growth of tomato seedlings to various degrees in the presence as well as in the absence of $NaHCO_3$ stress. Moreover, endogenous MT levels were low in leaves of the CK group and increased in the N group. The promotion of tomato seedling growth by exogenous MT application

was accompanied by increased endogenous MT content in the CK + MT and N + MT groups. This is consistent with the findings of Ren et al. [35], who reported that drought stress in maize resulted in increased MT levels in the roots and leaves compared with normal conditions. In a study of strawberry fruit ripening, Mansouri et al. [36] found that the increase in endogenous MT after exogenous MT injection may be related to the high expression of *TDC*, *SNAT*, *T5H*, and *ASMT*. They also suggested that this could be the reason for the accumulation of H_2O_2, due to the high expression of *NADPH* oxidase. This study is consistent with the findings of Sharafi, Y in tomato fruit. Sharafi, Y found that exogenous MT upregulates the expression of *TDC*, *T4H*, *SNAT*, and *ASMT* genes, which, in turn, promote the expression of signaling molecules responsible for endogenous MT accumulation [37]. In studies with wheat seedlings, exogenous application of MT mediated the expression of the *TaASMT1*, *TaASMT2*, and *TaTDC1* genes, which induced an increase in endogenous MT [38].

4.2. Effect of Exogenous MT Application on the pH of the Root Environment of Tomato Seedlings under $NaHCO_3$ Stress

Excessive pH mainly destroys the root system structure and leads to the loss of the normal physiological functions of root cells. Studies have reported that many plants are induced to secrete large amounts of acid to alter the pH of the root environment under saline and alkaline stresses, thus exerting a buffering effect to resist environmental changes to maintain normal cellular functioning [39]. In this study, MT application could reduce the pH of the root environment under alkali stress to some extent. Under control conditions, the root pH of tomato seedlings under CK + MT treatment was significantly lower than that of CK treatment, and the inter-root pH after $NaHCO_3$ treatment was significantly higher than that of the control. This showed that the high pH of the alkali-stress environment had changed the inter-root pH, which would lead to a decrease in root vigor and a change in osmotic pressure and, at the same time, disrupt the uptake of ions by the roots, while MT application could reduce the inter-root pH under alkali stress to a certain extent and, at the same time, disrupt the uptake of ions by the roots. The application of 100 $\mu mol \cdot L^{-1}$ MT caused a significant decrease in the pH under $NaHCO_3$ stress, which, in combination with the results of this study, could be used to determine the total organic acid content of tomato seedlings. The results of the total organic acid content measurements indicated that MT significantly increased the total acid content secreted by roots under unstressed conditions, whereas the total organic acid content was significantly reduced under N treatment. This indicates that MT treatment increased the amount of acid secretion by tomato seedlings, which, in turn, lowered the pH of the alkaline environmental conditions and mitigated the injury of the seedling root system caused by the high pH value.

In this study, oxalic acid was the main organic acid synthesized and secreted by tomato seedling roots under control conditions, which is consistent with the results of Xiang et al.'s study on organic acids in grape roots under salt stress [40]. In contrast, the content of oxalic acid significantly decreased but the content of succinic acid, citric acid, and malic acid significantly increased under stress conditions, suggesting that MT alleviates the growth of tomato seedlings under $NaHCO_3$ stress conditions and may improve tomato acclimatization to $NaHCO_3$ mainly by promoting the content of oxalic acid in the secreted organic acids in order to change the inter-root environment.

4.3. Effects of Exogenous MT on the Content of Photosynthetic Pigments and Photosynthetic Gas-Exchange Parameters in Tomato Seedlings under $NaHCO_3$ Stress

Photosynthesis is a critical and complex process that provides energy for plant metabolism. Accumulation of plant photosynthetic energy is closely related to chlorophyll synthesis, whereas accumulation of photosynthetic pigments is related to photosynthetic performance parameters. Chlorophyll synthesis is hampered by alkali stress, resulting in the yellowing of leaves, which leads to a decrease in the photosynthetic rate [41]. In this study, $NaHCO_3$ stress resulted in reduced chlorophyll content, which is consistent with the study by Liu et al. [21]. Exogenous application of MT resulted in a significant increase

in photosynthetic pigments; similar results were obtained by Li et al. [11]. The decrease in photosynthetic pigments in leaves under saline and alkali stresses could be attributed to the disruption of the chloroplast structure, which blocks chlorophyll synthesis. Wu et al. [20] reported that under salt and alkali stress conditions, cucumber seedlings had lower chlorophyll and carotenoid contents compared to the control. In our study, chlorophyll content was significantly increased after the exogenous application of MT under alkali stress, which may be due to the protective effect of exogenous MT on the stressed chloroplasts, slowing down the degradation of chlorophyll. Transcriptome studies indicate that MT also downregulates the expression of genes responsible for chlorophyll-degrading enzymes [42]. In this study, $NaHCO_3$ stress significantly decreased Pn, Gs, Tr, and Ci levels. This suggested that the main reason for the decrease in photosynthetic capacity of tomato seedlings due to alkali stress was stomatal limitation. MT treatment effectively increased the Pn, Gs, Tr, and Ci levels in tomato seedlings. This is consistent with the findings of Peng Ling et al. [43]. Exogenous MT treatment led to the improvement in the stomatal limitation of the photosynthetic rate under $NaHCO_3$ stress and increased the photosynthetic capacity of tomato seedlings.

4.4. Effect of Exogenous MT on Chlorophyll Fluorescence Parameters of Tomato Seedlings under $NaHCO_3$ Stress

Chlorophyll fluorescence is closely related to photosynthesis, and the state of the plant under stress can be visualized using a kinetic curve. The shape of its energy distribution is an indicator for evaluating the size of the pool of electron carriers in the photosynthetic electron-transport chain [44]. The conversion of light energy into chemical energy requires the joint participation of two light reaction systems, PSI and PSII. Damage to the photosystem leads to photoinhibition and low photosynthetic efficiency. Since electrons released from PSII are transferred to PSI in a linear electron flow, each step of the OJIP curve is related to the energy or linear electron-transfer efficiency between the PSII and PSI components [45]. Exogenously applied MT during chromium stress improves photochemical efficiency by protecting the OEC and PSII, thus protecting from stress-induced damage [46]. Exogenous MT application during drought can mitigate damage to the photosynthetic apparatus of maize by increasing the photosynthetic electron-transfer efficiency between the two photosystems and increasing the quantum yield of PSI and PSII photochemistry [47]. Under high-temperature stress, foliar spraying of MT maintained the structural integrity of the chloroplasts and cysts in *Chrysanthemum*, significantly reduced the increase in the K^- and J-points of the OJIP curve, and enhanced photosynthesis [48].

Our study demonstrated that $NaHCO_3$ stress caused the O-phase of the OJIP curve to rise, the P-phase to fall, the amplitude to decrease, the slope of its rise to gradually slow down, and the I−P phase to fall to the lowest among all treatments. This indicated that under $NaHCO_3$ stress, the PSII reaction center suffered damage or caused reversible inactivation, and that photoinhibition occurred in the tomato leaves, which led to decreased photosynthesis. After exogenous MT treatment (CK + MT), the O-phase of the OJIP curve of the leaves decreased and the P-phase increased; the I−P phase was significantly higher than that of tomato leaves under alkali treatment after spraying MT (N + MT) under alkali stress. The subsequent standardization of the OJIP curve revealed the appearance of the K-phase, which indicated that the OEC on the donor side of PSII was damaged, and that the efficiency of the electrons crossing the Q_A had decreased.

Combined with the fact that the PSII specific-activity parameters φR_o ψE_o, and ψR_o exhibited a decreasing trend, this indicates a gradual decrease in the PQ pool on the receptor side of the PSII reaction center in tomato seedlings under $NaHCO_3$ stress; a decrease in the overall functional activity of the electron-transport chain between PSII, PSI, and the whole system; and a significant decrease in the quantum efficiency activity of the terminal electron-acceptor reduction on the receptor side of the PSI receptor. The efficiency of the single exciton captured in the reaction center to drive all but Q_A electron transfer and the efficiency of individual electrons traveling from $Q_A{}^-$ through the electron-transport chain

to the terminal electron acceptor on the PSI receptor side significantly decreased. In contrast, the treatment with exogenous MT alleviated the injury to the OEC on the receptor side of PSII under alkali stress; increased the number of viable electrons in the reaction center; expanded the PQ pool; improved the rate and activity of electrons in the transfer process; optimized the allocation of light, excitation, and reduction energies in the reaction center; and reduced the heat dissipation. This facilitated the electron transfer on the receptor side of PSII and improved the alkali tolerance.

4.5. Effect of Exogenous MT on the Expression of Key Enzyme Genes of the Calvin Cycle in Tomato Seedlings under $NaHCO_3$ Stress Conditions

In C3 plants, the Calvin–Benson cycle (CBC) is the main pathway for photosynthetic CO_2 fixation, reduction, and regeneration [49]. Fructose-1,6-bisphosphate aldolase (*FBA*) is a key plant enzyme involved in glycolysis, gluconeogenesis, and the Calvin cycle, and increasing *FBA* increases the CO_2 concentration in plant tissues [50]. Fructose-1,6-bisphosphatase (*FBP*) catalyzes irreversible reactions during glycolysis and is involved in regulating the limiting factors of carbon flow through the Calvin cycle. Glyceraldehyde-3-phosphate dehydrogenase (*GAPDH*) is an enzyme involved in glucose metabolism during glycolysis and is considered a multifunctional protein [51]. MT increases expression of the *FBP* gene, which accelerates the Calvin cycle and further enhances carbon fixation, thereby promoting photosynthesis in kiwifruit seedlings under drought stress [52]. Moreover, MT regulates the expression of genes such as *ALDO*, *PGK*, *RCA*, *SBP*, and *PPC*, which encode enzymes in the reversible steps of the glycolysis and gluconeogenesis pathways. In our study, MT upregulated *FBA* and downregulated *GAPDH* and *FBP*. This suggested that MT can partially enhance glycolysis, inhibit gluconeogenesis, and gain more energy to counteract alkali stress. Studies have reported that the exogenous application of MT increases *SBP* enzyme activity, thereby improving the photosynthetic capacity and cold tolerance in tomato plants [53]. Exogenous MT reduces photoinhibition during cold storage in cucumber by regulating the expression of key genes in the Rubisco regeneration process and by maintaining a normal *CBC* [54]. *PRK* is a gene encoding a phosphokinase. The pentose phosphate pathway is the substrate of ribulose diphosphate carboxylase/oxygenase (Rubisco) in the Calvin cycle. Downregulation of the *PRK* gene decreases the photorespiration rate of the Rubisco enzyme, which oxygenates RuBP and promotes cyclic electron flow around PSI. *PGK* is the only enzyme in the Calvin cycle that has monomeric activity [55], and exogenous *SNP* increases *PGK* gene expression in tomato leaves under salt stress and alleviates injury caused by salt stress [25]. In our study, alkali stress upregulated *GAPDH* gene but downregulated *PGK*, *RCA*, and *SBP* genes in the leaves of tomato seedlings. This may be due to the initiation of a self-protection mechanism under adversity stress, which induced some enzyme genes. In contrast, exogenous MT significantly upregulated *FBA*, *FBP*, and *PGK* genes under alkali stress. This suggested that exogenous MT can regulate the upregulation of some key enzyme genes of the Calvin cycle, promote energy metabolism, and accelerate seedling growth. Therefore, exogenous MT sprayed under alkali stress could regulate the transcription level of Calvin-cycle-related genes, activate the genes involved in carbon metabolism, promote the conversion efficiency of carbon-assimilation-related metabolites, and accelerate the Calvin cycle, thus improving the photosynthetic efficiency and producing more energy and intermediates to enhance the tolerance to alkali stress. This may be an important mechanism by which MT enhances alkali tolerance in tomato seedlings.

In this study, we examined the impact of exogenously sprayed MT on tomato seedlings subjected to alkali stress, specifically with regard to plant growth, root pH, photosynthesis, and endogenous hormones. However, a transcriptomic analysis was not performed; therefore, in future studies, we plan to investigate the effects of exogenous MT on photosynthesis in tomato seedlings at the molecular level.

5. Conclusions

$NaHCO_3$ stress (60 mmol·L^{-1}) inhibited tomato seedling growth; decreased photosynthetic pigment content, photosynthetic performance, and photosynthetic electron transfer activity and efficiency; damaged the donor and acceptor sides of the photosynthetic electron-transport chain; and impaired photosynthetic capacity. In contrast, the exogenous application of MT alleviated the inhibitory effect of alkali stress on the growth of tomato seedlings, significantly increased the chlorophyll content and photosynthetic performance, upregulated the key genes encoding enzymes of the Calvin cycle, improved the efficiency of electron transfer, protected the OEC, and lowered the pH of the root environment. Therefore, MT can regulate the genes related to photosynthesis and carbon assimilation, improve leaf photosynthetic capacity, and regulate root pH, thereby promoting seedling growth and improving the alkali tolerance of tomato seedlings.

Author Contributions: Conceptualization, Y.Y. and S.G.; methodology, Y.Y., X.J. and S.G.; software, Y.Y. and M.L.; validation, Y.Y. and S.G.; formal analysis, Y.Y.; investigation, S.W. and M.D.; resources, Y.Y.; data curation, Y.Y., M.L. and X.J.; writing—original draft preparation, S.G. and S.W.; writing—review and editing, Y.Y.; visualization, X.J. and S.G.; supervision, M.D. and M.L.; project administration, M.D.; funding acquisition, M.D. All authors have read and agreed to the published version of the manuscript.

Funding: This work was funded by the "Mechanism of melatonin-induced tomato root acid exudation in promoting phosphorus utilization under sodic alkaline stress" (U1903105).

Institutional Review Board Statement: Not applicable.

Informed Consent Statement: Not applicable.

Data Availability Statement: Data are contained within the article.

Conflicts of Interest: Author Shaowei Wei is from Company National Water Saving Irrigation Engineering Technology Research Center,Xinjiang Tinaye Co., Ltd., Company National Water Saving Irrigation Engineering Technology Research Center,Xinjiang Tinaye Co., Ltd. had no role in the design of the study; in the collection, analyses, or interpretation of date; in the writing of manuscript, and in the decision to publish the results.

References

1. Manasa, M.R.K.; Katukuri, N.R.; Darveekaran Nair, S.S.; Haojie, Y.; Yang, Z.; Guo, R. bo Role of Biochar and Organic Substrates in Enhancing the Functional Characteristics and Microbial Community in a Saline Soil. *J. Environ. Manag.* **2020**, *269*, 110737. [CrossRef] [PubMed]
2. Yang, C.; Chong, J.; Li, C.; Kim, C.; Shi, D.; Wang, D. Osmotic Adjustment and Ion Balance Traits of an Alkali Resistant Halophyte Kochia Sieversiana during Adaptation to Salt and Alkali Conditions. *Plant Soil* **2007**, *294*, 263–276. [CrossRef]
3. Wang, J.; Zhang, Y.; Yan, X.; Guo, J. Physiological and Transcriptomic Analyses of Yellow Horn (*Xanthoceras sorbifolia*) Provide Important Insights into Salt and Saline-Alkali Stress Tolerance. *PLoS ONE* **2020**, *15*, e0244365. [CrossRef] [PubMed]
4. Wang, L.; Liu, N.; Wang, H.; Ren, J.; Yao, Y. Hydraulic properties and carbon metabolism of *Lycium barbarum* and *Tamarix tamarisk* under salinity stress. *J. Plant Sci.* **2017**, *35*, 865–873.
5. Li, N.; Zhang, Z.; Gao, S.; Lv, Y.; Chen, Z.; Cao, B.; Xu, K. Different Responses of Two Chinese Cabbage (*Brassica rapa* L. Ssp. Pekinensis) Cultivars in Photosynthetic Characteristics and Chloroplast Ultrastructure to Salt and Alkali Stress. *Planta* **2021**, *254*, 102. [CrossRef]
6. Wang, X.; Ren, H.; Wei, Z.; Wang, Y.; Ren, W. Effects of Neutral Salt and Alkali on Ion Distributions in the Roots, Shoots, and Leaves of Two Alfalfa Cultivars with Differing Degrees of Salt Tolerance. *J. Integr. Agric.* **2017**, *16*, 1800–1807. [CrossRef]
7. Wang, J.; Peng, X.; Gao, Y.; Wang, Y.; Lin, J.; Yan, X. Physiological and Proteomics Analyses Reveal the Resistance Response Mechanism to Alkali Stress in the Early Seedlings (Cotyledons vs. Roots) of Castor Plant (*Ricinus communis* L.). *Environ. Exp. Bot.* **2021**, *185*, 104414. [CrossRef]
8. Guo, J.J.; Xu, X.X.; Zhang, R.D.; Chen, X.F.; Xing, Y.F.; Li, B.; Liu, C.; Zhou, Y.F. Effect of Short-Term Combined Alkaline Stress on Antioxidant Metabolism, Photosynthesis, and Leaf-Air Temperature Difference in Sorghum. *Photosynthetica* **2022**, *60*, 200–211. [CrossRef]
9. Paredes, S.D.; Korkmaz, A.; Manchester, L.C.; Tan, D.-X.; Reiter, R.J. Phytomelatonin: A Review. *J. Exp. Bot.* **2009**, *60*, 57–69. [CrossRef]
10. Sun, C.; Liu, L.; Wang, L.; Li, B.; Jin, C.; Lin, X. Melatonin: A Master Regulator of Plant Development and Stress Responses. *J. Integr. Plant Biol.* **2021**, *63*, 126–145. [CrossRef]

11. Li, X.; Brestic, M.; Tan, D.-X.; Zivcak, M.; Zhu, X.; Liu, S.; Song, F.; Reiter, R.J.; Liu, F. Melatonin Alleviates Low PS I-Limited Carbon Assimilation under Elevated CO_2 and Enhances the Cold Tolerance of Offspring in Chlorophyll b-Deficient Mutant Wheat. *J. Pineal Res.* **2018**, *64*, e12453. [CrossRef] [PubMed]
12. Li, J.; Yang, Y.; Sun, K.; Chen, Y.; Chen, X.; Li, X. Exogenous Melatonin Enhances Cold, Salt and Drought Stress Tolerance by Improving Antioxidant Defense in Tea Plant (*Camellia sinensis* (L.) O. Kuntze). *Molecules* **2019**, *24*, 1826. [CrossRef] [PubMed]
13. Ramasamy, K.; Karuppasami, K.M.; Alagarswamy, S.; Shanmugam, K.P.; Rathinavelu, S.; Vellingiri, G.; Muniyappan, U.; Kanthan, T.; Kuppusamy, A.; Rajendran, M.; et al. Role of Melatonin in Directing Plant Physiology. *Agronomy* **2023**, *13*, 2405. [CrossRef]
14. Debnath, B.; Islam, W.; Li, M.; Sun, Y.; Lu, X.; Mitra, S.; Hussain, M.; Liu, S.; Qiu, D. Melatonin Mediates Enhancement of Stress Tolerance in Plants. *Int. J. Mol. Sci.* **2019**, *20*, 1040. [CrossRef]
15. Ma, S.; Gai, P.; Geng, B.; Wang, Y.; Ullah, N.; Zhang, W.; Zhang, H.; Fan, Y.; Huang, Z. Exogenous Melatonin Improves Waterlogging Tolerance in Wheat through Promoting Antioxidant Enzymatic Activity and Carbon Assimilation. *Agronomy* **2022**, *12*, 2876. [CrossRef]
16. Alyammahi, O.; Gururani, M.A. Chlorophyll-a Fluorescence Analysis Reveals Differential Response of Photosynthetic Machinery in Melatonin-Treated Oat Plants Exposed to Osmotic Stress. *Agronomy* **2020**, *10*, 1520. [CrossRef]
17. Li, Y.; Zhang, L.; Yu, Y.; Zeng, H.; Deng, L.; Zhu, L.; Chen, G.; Wang, Y. Melatonin-Induced Resilience Strategies against the Damaging Impacts of Drought Stress in Rice. *Agronomy* **2022**, *12*, 813. [CrossRef]
18. Zhou, X.; Zhao, H.; Cao, K.; Hu, L.; Du, T.; Baluška, F.; Zou, Z. Beneficial Roles of Melatonin on Redox Regulation of Photosynthetic Electron Transport and Synthesis of D1 Protein in Tomato Seedlings under Salt Stress. *Front. Plant Sci.* **2016**, *7*, 1823. [CrossRef]
19. Sun, S.; Wen, D.; Yang, W.; Meng, Q.; Shi, Q.; Gong, B. Overexpression of Caffeic Acid O-Methyltransferase 1 (COMT1) Increases Melatonin Level and Salt Stress Tolerance in Tomato Plant. *J. Plant Growth Regul.* **2020**, *39*, 1221–1235. [CrossRef]
20. Wu, P.; Lv, J.; Yu, J.; Liu, N.; Li, J.; Jing, L. Effects of melatonin on photosynthetic characteristics and osmoregulatory substance contents of cucumber seedlings under combined saline and alkaline stress. *J. Appl. Ecol.* **2022**, *33*, 1901–1910. [CrossRef]
21. Liu, N.; Jin, Z.; Wang, S.; Gong, B.; Wen, D.; Wang, X.; Wei, M.; Shi, Q. Sodic Alkaline Stress Mitigation with Exogenous Melatonin Involves Reactive Oxygen Metabolism and Ion Homeostasis in Tomato. *Sci. Hortic.* **2015**, *181*, 18–25. [CrossRef]
22. ElSayed, A.I.; Rafudeen, M.S.; Gomaa, A.M.; Hasanuzzaman, M. Exogenous Melatonin Enhances the Reactive Oxygen Species Metabolism, Antioxidant Defense-related Gene Expression, and Photosynthetic Capacity of *Phaseolus vulgaris* L. to Confer Salt Stress Tolerance. *Physiol. Plant.* **2021**, *173*, 1369–1381. [CrossRef] [PubMed]
23. Yin, Z.; Wang, Z.; Qi, M.; Meng, S.; Li, T. Effect of externally applied melatonin on photosynthetic function of tomato seedlings under salt stress. *J. Ecol.* **2019**, *38*, 467–475. [CrossRef]
24. Jiang, X.; Niu, N.; Cui, H.; Wei, S.; Xiong, H.; Liu, H.; Diao, M. Effect of foliar spraying of melatonin on photosynthetic characteristics of tomato seedlings under NaHCO3 stress. *Agric. Res. Arid Areas* **2022**, *40*, 87–95.
25. Li, X.; Wang, S.; Chen, X.; Cong, Y.; Cui, J.; Shi, Q.; Liu, H.; Diao, M. The Positive Effects of Exogenous Sodium Nitroprusside on the Plant Growth, Photosystem II Efficiency and Calvin Cycle of Tomato Seedlings under Salt Stress. *Sci. Hortic.* **2022**, *299*, 111016. [CrossRef]
26. Hao, H.; Chang, J.; Zhang, Z. Methods for studying plant root secretion. *Plant Physiol. Newsl.* **2003**, *39*, 56–60. [CrossRef]
27. Zhang, X.; Tan, G. *Experimental Techniques in Plant Physiology*; Liaoning Science and Technology Press: Shengyang, China, 1989.
28. Yan, Y.; Liu, X. A study of methods for the determination of chlorophyll. *J. Beijing Agric. Univ.* **1982**, *8*, 53–67.
29. Schansker, G.; Srivastava, A.; Strasser, R.J. Characterization of the 820-Nm Transmission Signal Paralleling the Chlorophyll a Fluorescence Rise (OJIP) in Pea Leaves. *Funct. Plant Biol.* **2003**, *30*, 785. [CrossRef]
30. Livak, K.J.; Schmittgen, T.D. Analysis of Relative Gene Expression Data Using Real-Time Quantitative PCR and the $2^{-\Delta\Delta CT}$ Method. *Methods* **2001**, *25*, 402–408. [CrossRef]
31. Ibrahim, M.F.M.; Elbar, O.H.A.; Farag, R.; Hikal, M.; El-Kelish, A.; El-Yazied, A.A.; Alkahtani, J.; El-Gawad, H.G.A. Melatonin Counteracts Drought Induced Oxidative Damage and Stimulates Growth, Productivity and Fruit Quality Properties of Tomato Plants. *Plants* **2020**, *9*, 1276. [CrossRef]
32. Altaf, M.A.; Shahid, R.; Ren, M.-X.; Altaf, M.M.; Jahan, M.S.; Khan, L.U. Melatonin Mitigates Nickel Toxicity by Improving Nutrient Uptake Fluxes, Root Architecture System, Photosynthesis, and Antioxidant Potential in Tomato Seedling. *J. Soil Sci. Plant Nutr.* **2021**, *21*, 1842–1855. [CrossRef]
33. Hu, E.; Liu, M.; Zhou, R.; Jiang, F.; Sun, M.; Wen, J.; Zhu, Z.; Wu, Z. Relationship between Melatonin and Abscisic Acid in Response to Salt Stress of Tomato. *Sci. Hortic.* **2021**, *285*, 110176. [CrossRef]
34. Siddiqui, M.H.; Khan, M.N.; Mukherjee, S.; Basahi, R.A.; Alamri, S.; Al-Amri, A.A.; Alsubaie, Q.D.; Ali, H.M.; Al-Munqedhi, B.M.A.; Almohisen, I.A.A. Exogenous Melatonin-mediated Regulation of K^+/Na^+ Transport, H^+-ATPase Activity and Enzymatic Antioxidative Defence Operate through Endogenous Hydrogen Sulphide Signalling in NaCl-stressed Tomato Seedling Roots. *Plant Biol. J.* **2021**, *23*, 797–805. [CrossRef] [PubMed]
35. Ren, J.; Yang, X.; Ma, C.; Wang, Y.; Zhao, J. Melatonin Enhances Drought Stress Tolerance in Maize through Coordinated Regulation of Carbon and Nitrogen Assimilation. *Plant Physiol. Biochem.* **2021**, *167*, 958–969. [CrossRef]
36. Mansouri, S.; Sarikhani, H.; Sayyari, M.; Soleimani Aghdam, M. Melatonin Accelerates Strawberry Fruit Ripening by Triggering GAMYB Gene Expression and Promoting ABA Accumulation. *Sci. Hortic.* **2021**, *281*, 109919. [CrossRef]

37. Sharafi, Y.; Aghdam, M.S.; Luo, Z.; Jannatizadeh, A.; Razavi, F.; Fard, J.R.; Farmani, B. Melatonin Treatment Promotes Endogenous Melatonin Accumulation and Triggers GABA Shunt Pathway Activity in Tomato Fruits during Cold Storage. *Sci. Hortic.* **2019**, *254*, 222–227. [CrossRef]
38. Ni, J.; Wang, Q.; Shah, F.A.; Liu, W.; Wang, D.; Huang, S.; Fu, S.; Wu, L. Exogenous Melatonin Confers Cadmium Tolerance by Counterbalancing the Hydrogen Peroxide Homeostasis in Wheat Seedlings. *Molecules* **2018**, *23*, 799. [CrossRef]
39. Robin, A.H.K.; Matthew, C.; Uddin, M.J.; Bayazid, K.N. Salinity-Induced Reduction in Root Surface Area and Changes in Major Root and Shoot Traits at the Phytomer Level in Wheat. *J. Exp. Bot.* **2016**, *67*, 3719–3729. [CrossRef]
40. Xiang, G.; Ma, W.; Gao, S.; Jin, Z.; Yue, Q.; Yao, Y. Transcriptomic and Phosphoproteomic Profiling and Metabolite Analyses Reveal the Mechanism of $NaHCO_3$-Induced Organic Acid Secretion in Grapevine Roots. *BMC Plant Biol* **2019**, *19*, 383. [CrossRef]
41. Gong, B.; Li, X.; VandenLangenberg, K.M.; Wen, D.; Sun, S.; Wei, M.; Li, Y.; Yang, F.; Shi, Q.; Wang, X. Overexpression of S-adenosyl-L-methionine Synthetase Increased Tomato Tolerance to Alkali Stress through Polyamine Metabolism. *Plant Biotechnol. J.* **2014**, *12*, 694–708. [CrossRef]
42. Wei, W.; Li, Q.-T.; Chu, Y.-N.; Reiter, R.J.; Yu, X.-M.; Zhu, D.-H.; Zhang, W.-K.; Ma, B.; Lin, Q.; Zhang, J.-S.; et al. Melatonin Enhances Plant Growth and Abiotic Stress Tolerance in Soybean Plants. *J. Exp. Bot.* **2015**, *66*, 695–707. [CrossRef] [PubMed]
43. Peng, L.; Li, A.; Yang, M.; Song, B.; Gao, Y.; Li, H. Effects of externally applied melatonin on growth and physiological characteristics of safflower under salt stress. *Chin. Herb. Med.* **2019**, *42*, 1730–1737. [CrossRef]
44. Zivcak, M.; Brestic, M.; Kunderlikova, K.; Olsovska, K.; Allakhverdiev, S.I. Effect of Photosystem I Inactivation on Chlorophyll a Fluorescence Induction in Wheat Leaves: Does Activity of Photosystem I Play Any Role in OJIP Rise? *J. Photochem. Photobiol. B Biol.* **2015**, *152*, 318–324. [CrossRef] [PubMed]
45. Tikkanen, M.; Rantala, S.; Aro, E.-M. Electron Flow from PSII to PSI under High Light Is Controlled by PGR5 but Not by PSBS. *Front. Plant Sci.* **2015**, *6*, 521. [CrossRef]
46. Ayyaz, A.; Amir, M.; Umer, S.; Iqbal, M.; Bano, H.; Gul, H.S.; Noor, Y.; Kanwal, A.; Khalid, A.; Javed, M.; et al. Melatonin Induced Changes in Photosynthetic Efficiency as Probed by OJIP Associated with Improved Chromium Stress Tolerance in Canola (*Brassica napus* L.). *Heliyon* **2020**, *6*, e04364. [CrossRef]
47. Guo, Y.Y.; Li, H.J.; Liu, J.; Bai, Y.W.; Xue, J.Q.; Zhang, R.H. Melatonin Alleviates Drought-Induced Damage of Photosynthetic Apparatus in Maize Seedlings. *Russ. J. Plant Physiol.* **2020**, *67*, 312–322. [CrossRef]
48. Qi, X.-Y.; Wang, W.-L.; Hu, S.-Q.; Liu, M.-Y.; Zheng, C.-S.; Sun, X.-Z. Effects of Exogenous Melatonin on Photosynthesis and Physiological Characteristics of Chry-Santhemum Seedlings under High Temperature Stress. *Ying Yong Sheng Tai Xue Bao* **2021**, *32*, 2496–2504. [CrossRef]
49. Michelet, L.; Zaffagnini, M.; Morisse, S.; Sparla, F.; Pérez-Pérez, M.E.; Francia, F.; Danon, A.; Marchand, C.H.; Fermani, S.; Trost, P.; et al. Redox Regulation of the Calvin–Benson Cycle: Something Old, Something New. *Front. Plant Sci.* **2013**, *4*, 470. [CrossRef]
50. Lv, G.-Y.; Guo, X.-G.; Xie, L.-P.; Xie, C.-G.; Zhang, X.-H.; Yang, Y.; Xiao, L.; Tang, Y.-Y.; Pan, X.-L.; Guo, A.-G.; et al. Molecular Characterization, Gene Evolution, and Expression Analysis of the Fructose-1, 6-Bisphosphate Aldolase (FBA) Gene Family in Wheat (*Triticum aestivum* L.). *Front. Plant Sci.* **2017**, *8*, 1030. [CrossRef]
51. Tristan, C.; Shahani, N.; Sedlak, T.W.; Sawa, A. The Diverse Functions of GAPDH: Views from Different Subcellular Compartments. *Cell. Signal.* **2011**, *23*, 317–323. [CrossRef]
52. Liang, D.; Ni, Z.; Xia, H.; Xie, Y.; Lv, X.; Wang, J.; Lin, L.; Deng, Q.; Luo, X. Exogenous Melatonin Promotes Biomass Accumulation and Photosynthesis of Kiwifruit Seedlings under Drought Stress. *Sci. Hortic.* **2019**, *246*, 34–43. [CrossRef]
53. Ding, F.; Liu, B.; Zhang, S. Exogenous Melatonin Ameliorates Cold-Induced Damage in Tomato Plants. *Sci. Hortic.* **2017**, *219*, 264–271. [CrossRef]
54. Zhao, H.; Zhang, Z.; Zhang, Y.; Bai, L.; Hu, X.; Li, X.; Zhang, L.; Miao, Y.; Wang, Y. Melatonin Reduces Photoinhibition in Cucumber during Chilling by Regulating the Calvin-Benson Cycle. *Sci. Hortic.* **2022**, *299*, 111007. [CrossRef]
55. Sharma, S.; Joshi, J.; Kataria, S.; Verma, S.K.; Chatterjee, S.; Jain, M.; Pathak, K.; Rastogi, A.; Brestic, M. Chapter 27—Regulation of the Calvin Cycle under Abiotic Stresses: An Overview. In *Plant Life under Changing Environment*; Tripathi, D.K., Pratap Singh, V., Chauhan, D.K., Sharma, S., Prasad, S.M., Dubey, N.K., Ramawat, N., Eds.; Academic Press: Cambridge, MA, USA, 2020; pp. 681–717. ISBN 978-0-12-818204-8.